

REVIEW ARTICLE

# Non-Invasive Diagnosis of Abdomino-Pelvic Masses: Role of Multimodality Imaging

Vijayanadh Ojili, Sree Harsha Tirumani<sup>1</sup>, Kedar N. Chintapalli, Gowthaman Gunabushanam<sup>2</sup>

Department of Radiology, University of Texas Health Sciences Centre at San Antonio, San Antonio, TX 78229, <sup>1</sup>Department of Imaging, Dana Farber Cancer Institute, Harvard Medical School, Boston, MA 02215, <sup>2</sup>Department of Diagnostic Radiology, Yale University School of Medicine, New Haven, Connecticut, 06520-8042, USA

**Address for correspondence:**

Dr. Vijayanadh Ojili  
 Department of Radiology, University of Texas Health Science Center at San Antonio, USA.  
**E-mail:** [ojili@uthscsa.edu](mailto:ojili@uthscsa.edu)



**Received :** 05-11-2012  
**Accepted :** 18-12-2012  
**Published :** 30-01-2013

## ABSTRACT

Recent advances in radiology have greatly increased the ability to make highly accurate diagnosis. Biopsy of many commonly seen lesions is no longer performed as the radiological findings are pathognomonic. This gives rise to the concept of 'virtual biopsy', a term coined on the lines of other imaging techniques such as virtual colonoscopy. Virtual biopsy is not a new imaging technique but a new concept which refers to the use of existing imaging modalities to evaluate the morphological features of tumors and arriving at a non-invasive diagnosis with a high degree of confidence obviating the need for true biopsy. Elements of virtual biopsy have already been incorporated into some evidence-based guidelines, and it is expected that with further technological advancements, an increasing number of tumors may be diagnosed and managed accordingly. A wider acceptance of virtual biopsy could further reduce the need for invasive biopsies and its attendant costs and risks. In this review article, we use index cases to further emphasize this concept.

**Key words:** Abdomen, computed tomography, magnetic resonance imaging, ultrasound, virtual biopsy

## INTRODUCTION

The ultimate goal of radiology is to make an accurate diagnosis noninvasively that reflects the underlying pathological condition. With recent advances in imaging

techniques, availability of novel contrast agents and better understanding of the pathophysiological basis of disease processes, radiological diagnoses can be made with such a high degree of accuracy in some conditions that an invasive biopsy is almost never warranted. This has the potential to give rise to the radiological concept of 'virtual biopsy'. Virtual biopsy, unlike virtual colonoscopy is not a new imaging technique, but a different way of looking at the existing imaging modalities and their diagnostic capabilities. It refers to the use of existing imaging techniques to evaluate the morphological features of tumors and arriving at a non-invasive diagnosis with a high degree of confidence. The key to making such an accurate diagnosis lie in

Access this article online	
Quick Response Code:	Website: <a href="http://www.clinicalimagingscience.org">www.clinicalimagingscience.org</a>
	DOI: 10.4103/2156-7514.106621

Copyright: © 2013 Ojili V. This is an open-access article distributed under the terms of the Creative Commons Attribution License, which permits unrestricted use, distribution, and reproduction in any medium, provided the original author and source are credited.

This article may be cited as:  
 Ojili V, Tirumani SH, Chintapalli KN, Gunabushanam O. Non-Invasive Diagnosis of Abdomino-Pelvic Masses: Role of Multimodality Imaging. J Clin Imaging Sci 2013;3:6.  
 Available FREE in open access from: <http://www.clinicalimagingscience.org/text.asp?2013/3/1/6/106621>

understanding the correlation between radiological and histomorphological features of tumors. A close attention to the fine details on imaging and prudent use of combination of imaging modalities form the basis for the future of virtual biopsy. Already, evidence-based guidelines such as the Royal College of Radiologists referral guidelines, the American College of Radiology (ACR) appropriateness criteria for adrenal tumors, and the American Association for the Study of Liver Diseases (AASLD) practice guidelines for hepatocellular carcinoma (HCC), incorporate elements of the virtual biopsy concept. Further familiarizing general practitioners and non-radiology specialists with this concept may help avoid unnecessary referrals for biopsy and additional work-up. In this review, we use few illustrative examples to show conditions where a virtual biopsy is possible due to highly accurate radiological diagnosis, thereby obviating the need for an invasive biopsy.

## LIVER

### Hemangioma

Hemangioma is the most common benign solid liver lesion and often incidentally detected in asymptomatic women, unless very large in size, when it may cause symptoms due to its size and pressure. Typical hemangioma is seen on ultrasound (US) as a well-defined hyperechoic lesion with posterior acoustic enhancement, while on dynamic computed tomography (CT), it demonstrates peripheral nodular enhancement with progressive centripetal filling. At magnetic resonance (MR) imaging, it typically has low signal on T1-weighted and high signal on T2-weighted sequences, retaining high signal on long TE sequences. It appears bright on diffusion weighted images (DWI) with mean apparent diffusion co-efficient (ADC) values usually between cysts and HCC; however, there can be significant overlap.<sup>[1]</sup> Enhancement on post gadolinium images is identical to CT, with no uptake of hepatocyte specific agents. Typical hemangiomas are diagnosed with 99% accuracy, 98% sensitivity and specificity and almost never biopsied.<sup>[2]</sup>

### Hepatic adenoma

Hepatic adenoma is an uncommon benign tumor occurring in young women, associated with the use of steroids and Type I glycogen storage disorder. On histology, adenoma is composed of lipid and glycogen rich hepatocytes with predominant hepatic arterial supply and no biliary channels or functioning Kupffer cells.<sup>[3]</sup> Hemorrhage is common due to thin walled sinusoids, poor connective tissue, and absence of a capsule.<sup>[3]</sup>

The imaging features of hepatic adenomas are determined by their three important histologic hallmarks: Lipid-rich cells, hepatic arterial supply, and absence of biliary channels.

The hyperechoic and often heterogeneous appearance of adenomas on US [Figure 1a] is due to their lipid content and hemorrhage.<sup>[3]</sup> Doppler US may show peripheral and intratumoral vessels with low resistance flow reflecting their hepatic arterial supply.<sup>[3]</sup> Unenhanced CT demonstrates an iso-, or less commonly hypo- or hyper-attenuating lesion relative to the liver parenchyma depending on lipid content and hemorrhage. Dynamic CT shows hypervascular lesion in the hepatic arterial phase which is iso-attenuating in the venous phase [Figure 1b and c].<sup>[3]</sup> CT also demonstrates complications such as hemorrhage and rupture [Figure 1d]. At MR, adenoma may be hypo-, iso- or hyperintense on T1-weighted images and predominantly high signal on T2-weighted images.<sup>[3]</sup> High T1-weighted signal seen in 35% of adenomas may be due to lipid or hemorrhage.<sup>[3]</sup> Delayed phase imaging shows no enhancement with Gd-BOPTA but variable enhancement with Gd-EOB-DTPA.<sup>[4,5]</sup>

### Focal nodular hyperplasia

Focal nodular hyperplasia (FNH) is the second most common benign liver tumor. It is more common in women and develops as a hyperplastic reaction to vascular malformations. Classic FNH is characterized by abnormal nodular architecture, cholangiolar proliferation and malformed vessels whereas the non-classic type lacks either the nodular architecture or malformed vessels but always contain biliary channels.<sup>[6]</sup> The presence of biliary channels which are dysfunctional is exploited in making a sensitive diagnosis of FNH.



**Figure 1:** Multiple hepatic adenomas. (a) Transverse ultrasound image of the left lobe of the liver shows a heterogeneous, predominantly hyperechoic lesion (arrow) with no overlying liver parenchyma. Another hypoechoic lesion (arrow head) is seen anteriorly. (b and c) Axial contrast-enhanced computed tomography (CT) sections of the liver in (b) hepatic arterial and (c) portal venous phases reveal hypervascular lesions (white arrows and arrowhead) in the left lobe of the liver which are isodense on the venous phase. Note the absence of capsule and peripheral liver parenchyma. Small incidental left renal angiomyolipomas (double lined arrows in c) are also noted. A diagnosis of multiple hepatic adenomas was made. (d) Axial contrast-enhanced CT image demonstrates rupture of the hepatic adenoma (arrow) with perihepatic hematoma. The patient was initially managed with hepatic artery embolization and the lesions were subsequently excised surgically with histopathology confirming adenomas.

The imaging hallmark of FNH is their close resemblance to the normal hepatic parenchyma. FNH is often seen as a subtle change in echogenicity compared to surrounding liver parenchyma with a hypoechoic halo of surrounding compressed parenchyma in some cases.<sup>[6]</sup> On CT [Figure 2], FNH is usually isodense on unenhanced images and hyperdense on the arterial phase, becoming isoattenuating to the surrounding liver in the venous phase. Classic FNH has a central scar which is hypodense and enhances on the delayed phase.<sup>[6]</sup> On magnetic resonance imaging (MRI), FNH is iso- or hypo-intense on T1 and hyper- or iso-intense on T2-weighted images, shows intense homogenous enhancement on arterial phase, becoming iso-intense on venous phase [Figure 3].<sup>[6]</sup> The central scar is usually hyper-intense on T2-weighted images and may show enhancement on delayed imaging.<sup>[6]</sup> FNH shows uptake of hepatocyte specific agents like gadoxetate disodium (Gd-EOB-DTPA) due to presence of functioning hepatocytes and appears iso- or hyper-intense due to trapping of the contrast in the aberrant bile ducts [Figure 3].<sup>[7]</sup> Sensitivity and specificity for MRI in characterizing FNH is 70% and 98% respectively.<sup>[6]</sup>

### Hepatocellular carcinoma

Hepatocellular carcinoma (HCC) is the most common primary malignant liver tumor and usually occurs in the setting of cirrhosis and chronic hepatitis B and C



**Figure 2:** Focal nodular hyperplasia. (a and b) Axial contrast-enhanced computed tomography sections of the liver in (a) hepatic arterial and (b) portal venous phase demonstrate a focal lesion (arrow) in the right lobe which is hypervascular in the arterial phase and becomes iso- to hypo-dense to the liver parenchyma in the venous phase.

infections. Earlier detection of HCC allows initiation of curative therapy and for this, surveillance in cirrhotic patients is performed with alpha-fetoprotein testing and sonography.<sup>[8]</sup> Sonographic features of HCC are variable with sensitivity as low as 20.5%<sup>[9]</sup> to as high as 81%.<sup>[10]</sup> Dynamic CT demonstrates HCC as a hypervascular lesion with abnormal intra-tumoral vessels in the arterial phase, which becomes iso-hypoattenuating on the venous phase images due to washout.<sup>[11]</sup>

At MRI, HCC is usually hypointense on T1-weighted and intermediate to high signal on T2-weighted images [Figure 4]. Small (<2 cm) HCC can be isointense on both T1 and T2-weighted images.<sup>[12]</sup> Dynamic gadolinium-enhancement shows hyper-vascular lesion in the arterial phase with washout in the venous phase and enhancing capsule in the delayed phase [Figure 4].<sup>[12]</sup> The predominant arterial supply of HCC in contrast to the predominant portal venous supply of normal hepatic parenchyma allows prompt detection of hyper-vascular HCC and underscores the need for good arterial phase imaging. Washout in the venous phase helps in differentiating HCC from dysplastic nodule and has sensitivity and specificity of 89% and 96% respectively.<sup>[12]</sup> At DWI, HCC shows restriction of diffusion with low ADC values.<sup>[13]</sup> HCC shows variable uptake of hepatocyte specific contrast agents depending on the degree of differentiation.<sup>[14]</sup> Portal vein thrombus that shows neovascularity and appears hyperintense on T2-weighted images and shows enhancement on dynamic imaging suggests tumor thrombus rather than bland thrombus.<sup>[12]</sup> Pooled sensitivity and specificity of MRI for HCC detection are 81% and 85% compared to 68% and 93% contrast enhanced spiral CT.<sup>[12]</sup> Double contrast MR imaging with gadolinium-based and iron oxide particles has sensitivity of 92% for detecting HCC of 1-2 cm size.<sup>[12]</sup> According to the AASLD practice guidelines, for a lesion >2 cm in a cirrhotic liver, biopsy is not essential if there are typical imaging features in one dynamic imaging study and for lesions between 1 cm and 2 cm, biopsy is not essential if

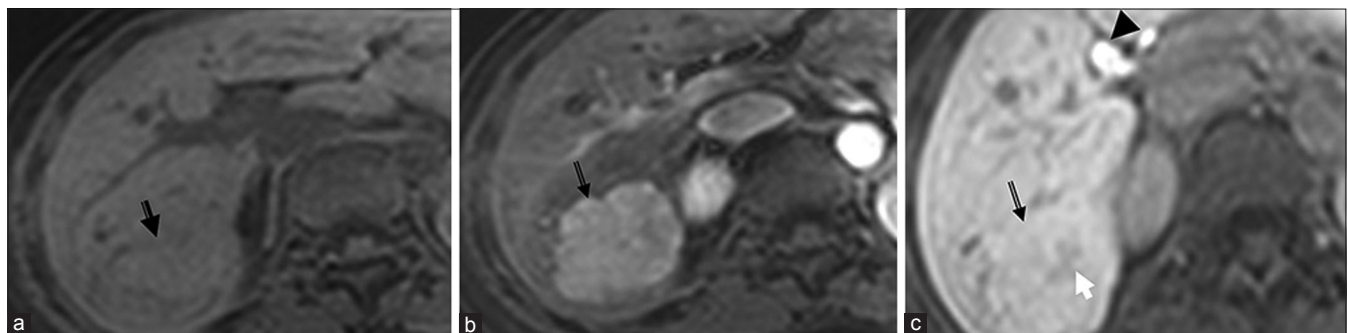


**Figure 3:** Focal nodular hyperplasia. (a, b and c) Dynamic contrast-enhanced magnetic resonance imaging with Gadaxetate disodium (Gd-EOB-DTPA) on T1-weighted images (a) Arrow emonstrates an isointense lesion. (b) in arterial phase it is hypervascular and (c) on 20 min delayed phase retains contrast. Note the central scar (white arrow) and contrast excretion in the biliary tree (arrow head) on the delayed image (c).

there are typical imaging features on two dynamic imaging studies.<sup>[15]</sup>

## RENAL TUMORS

### Renal cell carcinoma

Renal cell carcinoma (RCC) is the most common primary malignancy of the kidney and commonly affects men in their fifth to seventh decades. Three major types of RCC which differ in clinical behavior and treatment response include clear cell (80%), papillary (15%) and chromophobe (5%).<sup>[16]</sup> Clear cell carcinoma is composed of large uniform cells with abundant clear cytoplasm rich in glycogen and lipid.<sup>[17]</sup>

Clear cell RCC on sonography appears as a hypoechoic or complex solid cystic mass with thick septations. On CT, clear cell variant, owing to its hypervascularity, has the highest attenuation and enhancement in the corticomedullary and nephrographic phases distinguishing it from other types.<sup>[17,18]</sup> It is hypo- to isointense on T1-weighted MR images and iso-hyperintense on T2-weighted images with greater percentage enhancement than other phenotypes on dynamic contrast enhanced MRI [Figure 5]. The presence of lipid-rich cells is taken advantage of by using chemical shift imaging. The intra-tumoral lipid vacuoles result in a characteristic signal drop on opposed-phase MR images, which has a sensitivity of 42-84% and specificity of 94-100% [Figure 5].<sup>[16]</sup>

### Renal angiomyolipoma

Renal angiomyolipoma (Renal AML) is a hamartomatous mesenchymal tumor with 80% occurring as isolated sporadic cases and 20% in association with tuberous sclerosis.<sup>[19]</sup> AML is typically seen as a well-defined hyperechoic mass on US and as a noncalcified cortical tumor with macroscopic fat on CT [Figure 6].<sup>[19]</sup> At MRI, it has high signal on T1-weighted images with loss of signal on fat-suppressed sequences and variable signal on T2-weighted images due to intra-tumoral soft-tissue, which indicates vascular and smooth muscle components and hemorrhage.<sup>[19]</sup>

### Adrenal tumors

Evidence based approach to adrenal lesions resulted in the development of various criteria to make a confident diagnosis of adrenal lesions. ACR appropriateness criteria recommend biopsy only after a lesion is indeterminate on all imaging modalities.<sup>[20]</sup> Unenhanced CT attenuation of less than 10 HU, presence of intra-voxel lipid, adrenal to spleen signal intensity ratio of less than 0.71 and adrenal signal intensity index of 16.5% on MRI are virtually diagnostic of lipid rich adenoma [Figure 7].<sup>[21]</sup> On dynamic contrast enhanced CT, an absolute washout

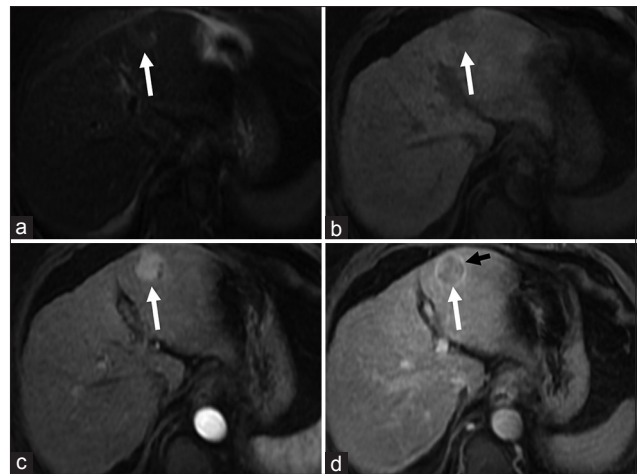


**Figure 4:** Hepatocellular carcinoma (a) Axial T2-weighted magnetic resonance (MR) image demonstrates a hyperintense lesion (arrow) in the segment III of the liver. Axial fat-suppressed (b) pre and post-gadolinium T1-weighted MR images in the (c) arterial and (d) delayed phases reveal the lesion to be faintly hypointense and hypervascular with washout in the delayed phase. Note the enhancing peripheral tumor capsule on delayed images (black arrow in d).

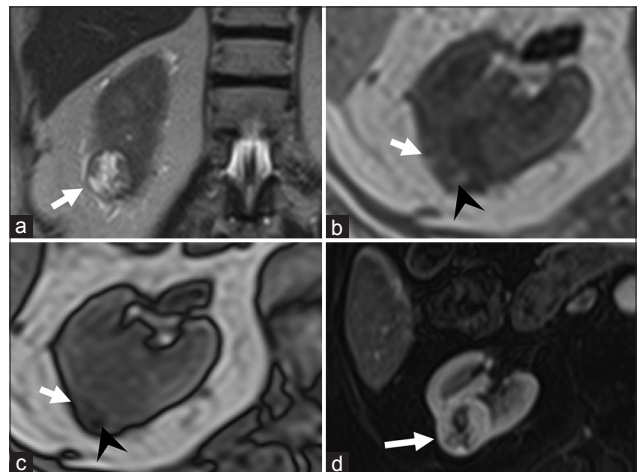


**Figure 5:** Clear cell variant of renal cell carcinoma. (a) Coronal T2-weighted magnetic resonance (MR) image demonstrates a hyperintense lesion (arrow) in the lower pole of right kidney. Axial (b) in- and (c) out-of-phase T1-weighted MR images demonstrate areas of drop in signal (arrow head) in the lesion suggestive of intra-lesional fat. (d) Axial fat-suppressed post-gadolinium T1-weighted MR image in the arterial phase reveals the lesion to be hypervascular. Histopathology confirmed clear cell variant of renal cell carcinoma.

of more than 60% or relative washout of more than 40% on 15 min delayed scans are diagnostic of lipid poor adenomas.<sup>[21]</sup> An absolute enhancement of more than 110-120 HU is diagnostic of pheochromocytoma regardless of washout.<sup>[22]</sup> Presence of macroscopic fat is diagnostic of myelolipoma [Figure 8].

## UTERUS AND OVARIES

Lipoleiomyomas are unusual types of leiomyomas resulting from fatty metamorphosis of smooth muscle cells of leiomyomas, with a reported incidence of 0.03-0.2%.<sup>[23]</sup> Histologically, they are composed of abundant fat within the myomatous tissue. US shows

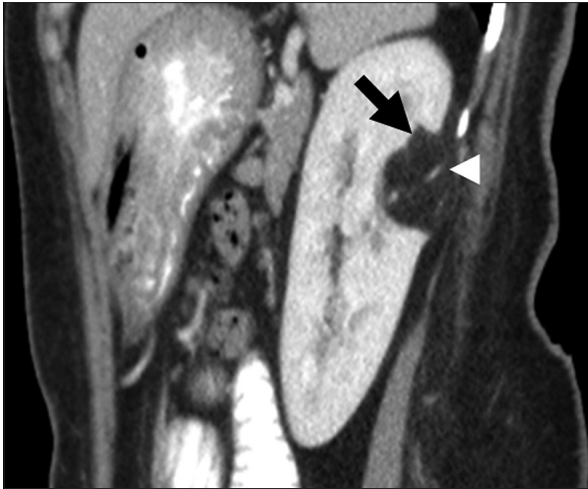


**Figure 6:** Renal angiomyolipoma. Sagittal reformatted image of contrast enhanced computed tomography shows a fat attenuation lesion (black arrow) in the posterior interpolar region of the left kidney. Note the prominent vascular component (arrow head) in the lesion.

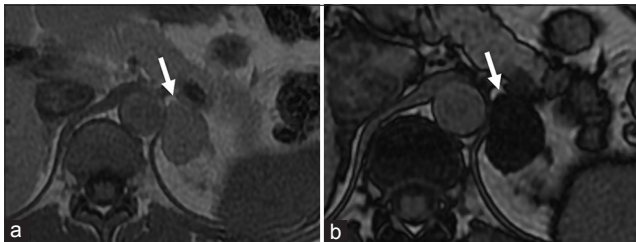


**Figure 7:** Adrenal Adenoma. Axial (a) in- and (b) out-of-phase T1-weighted magnetic resonance images demonstrate (a) left adrenal lesion (arrow) which shows significant drop of signal in the out-of-phase image (b) suggestive of lipid-rich adenoma.

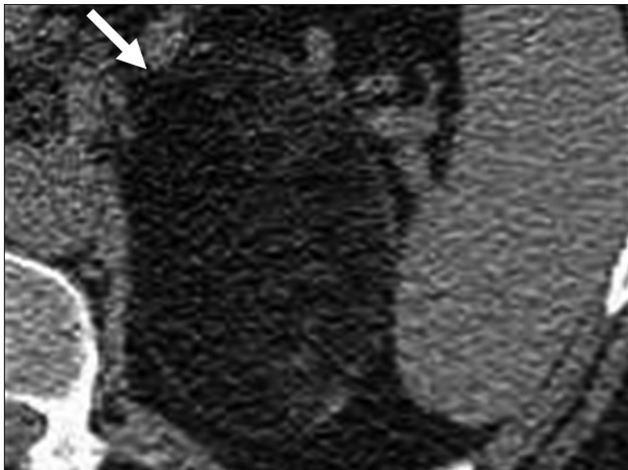


**Figure 8:** Adrenal myelolipoma. Axial unenhanced computed tomography shows a well-defined lesion with macroscopic fat (arrow) in the left suprarenal region.

a predominantly hyperechoic myometrial mass with peripheral hypoechoic rind in contrast to non-degenerated fibroids, which are hypoechoic [Figure 9a]. CT demonstrates a well-circumscribed myometrial lesion with macroscopic fat [Figure 9b].<sup>[24]</sup> On MR, the fat component has high signal

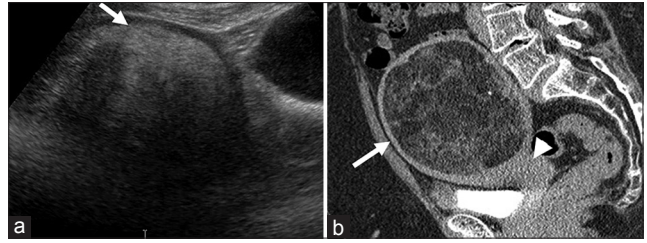


**Figure 9:** Uterine lipoleiomyoma: (a) Sagittal ultra sound image through the pelvis demonstrates a heterogeneous, predominantly hyperechoic lesion (arrow). (b) Sagittal reformatted computed tomography image of the pelvis reveals the mass to be arising from the uterus (arrow head) and contain macroscopic fat (arrow).



**Figure 10:** Ovarian teratoma. Axial contrast-enhanced computed tomography image of the pelvis reveals a well-defined adnexal lesion with fat (single arrow), fat-fluid level (arrow head) and calcification (double arrow).

on T1-weighted images that is suppressed on fat saturated sequences.<sup>[23]</sup>

Some ovarian tumors have typical imaging features that allow for a highly specific diagnosis to be made. Ovarian teratoma, the most common germ cell tumor of the ovary, has several histological types based on the degree of differentiation. Mature teratoma is composed of tissues derived from two or more germ cell layers. Pathologically, it is a unilocular (88%) cystic lesion composed of sebaceous material and squamous epithelial lining with a raised nodule (Rokitansky nodule) and various other structures like hair follicles, cutaneous glands and muscle.<sup>[25]</sup> Mature teratoma is seen on sonography as a cystic lesion with echogenic tubercle, diffusely echogenic mass or cystic lesion with echogenic septa.<sup>[25]</sup> At CT, presence of fat attenuation in an adnexal cyst with or without calcification and fluid level is diagnostic [Figure 10].<sup>[25]</sup> The sebaceous component of teratoma has high signal on T1-weighted images matching retroperitoneal fat and variable signal on T2-weighted images with marked signal loss on fat saturated images [Figure 11].

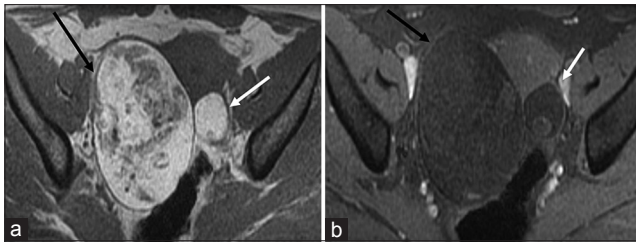


**Figure 11:** Ovarian teratoma. Axial non-fat-suppressed (a) pre- and (b) fat-suppressed post-gadolinium T1-weighted magnetic resonance images demonstrate high signal intensity areas in the lesion (a) on non-fat-suppressed image which are suppressed on the fat-suppressed image suggestive of macroscopic fat in the lesion (black arrow). Note the presence of a smaller teratoma in the left ovary which shows similar signal characteristics (white arrow).

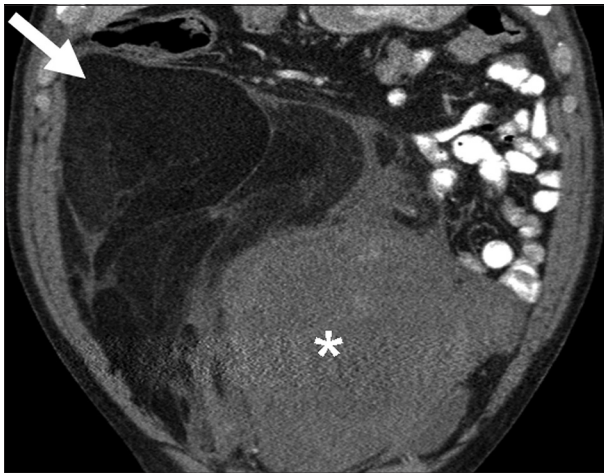


**Figure 12:** Retroperitoneal liposarcoma. Coronal reformatted image of contrast-enhanced computed tomography demonstrates a large retroperitoneal mass with areas of fatty attenuation (single arrow) and heterogeneous soft tissue component (asterisk).

## MISCELLANEOUS

Lipomas are benign fat containing tumors whereas well differentiated liposarcomas are uncommon malignant fat containing tumors. Lipomas can be treated by simple enucleation whereas liposarcomas need wide local excision and long follow up due to high risk of recurrence and dedifferentiation.<sup>[26]</sup> Simple lipomas do not pose a significant diagnostic dilemma; they appear as encapsulated homogenous fat attenuation lesions on CT and bright T1-weighted and intermediate signal T2-weighted lesions on MRI with occasional smooth septa.<sup>[26,27]</sup> These findings are 100% specific for diagnosis of simple lipomas.<sup>[26]</sup> Well differentiated liposarcomas are characterized by the presence of thick, irregular septa, nodular and/or globular regions of non-adipose tissue within the lesion, total amount of non-adipose tissue composing more than 25% of the lesion and prominent areas of enhancement on both CT and MRI [Figure 12].<sup>[28]</sup> In one study, these findings were 100% sensitive and 83% specific for diagnosis of well differentiated liposarcomas.<sup>[26]</sup>

## CONCLUSION

In conclusion, a clear understanding and correlation of the histopathologic and imaging features of certain tumors can help in avoiding an invasive biopsy. Occasionally, a combination of imaging modalities may be required to achieve greater diagnostic certainty. We believe that with further advancements in radiology hardware and the development of tissue specific contrast agents, an increased number of pathological entities may be diagnosed by virtual biopsy. Finally, a greater emphasis on evidence based guidelines could result in the development of more imaging workup algorithms, potentially strengthening the idea of virtual biopsy.

## REFERENCES

1. Taouli B, Vilgrain V, Dumont E, Daire JL, Fan B, Menu Y. Evaluation of liver diffusion isotropy and characterization of focal hepatic lesions with two single-shot echo-planar MR imaging sequences: Prospective study in 66 patients. *Radiology* 2003;226:71-8.
2. Maniam S, Szklaruk J. Magnetic resonance imaging: Review of imaging techniques and overview of liver imaging. *World J Radiol* 2010;2:309-22.
3. Kamaya A, Maturen KE, Tye GA, Liu YI, Parti NN, Desser TS. Hypervascular liver lesions. *Semin Ultrasound CT MR* 2009;30:387-407.
4. Grazioli L, Morana G, Kirchin MA, Schneider G. Accurate differentiation of focal nodular hyperplasia from hepatic adenoma at gadobenate dimeglumine-enhanced MR imaging: Prospective study. *Radiology* 2005;236:166-77.
5. Ringe KI, Husarik DB, Sirlin CB, Merkle EM. Gadoxetate disodium-enhanced MRI of the liver: Part 1, protocol optimization and lesion appearance in the noncirrhotic liver. *AJR Am J Roentgenol* 2010;195:13-28.
6. van den Bos IC, Hussain SM, de Man RA, Zondervan PE, Ijzermans JN, Krestin GP. Primary hepatocellular lesions: Imaging findings on state-of-the-art magnetic resonance imaging, with pathologic correlation. *Curr Probl Diagn Radiol* 2008;37:104-14.
7. Grazioli L, Bondioni MP, Haradome H, Motosugi U, Tinti R, Frittoli B, et al. Hepatocellular adenoma and focal nodular hyperplasia: Value of gadoteric acid-enhanced MR imaging in differential diagnosis. *Radiology* 2012;262:520-9.
8. Aghoram R, Cai P, Dickinson JA. Alpha-fetoprotein and/or liver ultrasonography for screening of hepatocellular carcinoma in patients with chronic hepatitis B. *Cochrane Database Syst Rev* 2012;9:CD002799.
9. Bennett GL, Krinsky GA, Abitbol RJ, Kim SY, Theise ND, Teperman LW. Sonographic detection of hepatocellular carcinoma and dysplastic nodules in cirrhosis: Correlation of pretransplantation sonography and liver explant pathology in 200 patients. *AJR Am J Roentgenol* 2002;179:75-80.
10. Miller WJ, Federle MP, Campbell WL. Diagnosis and staging of hepatocellular carcinoma: Comparison of CT and sonography in 36 liver transplantation patients. *AJR Am J Roentgenol* 1991;157:303-6.
11. Furlan A, Marin D, Vanzulli A, Patera GP, Ronzoni A, Midiri M, et al. Hepatocellular carcinoma in cirrhotic patients at multidetector CT: Hepatic venous phase versus delayed phase for the detection of tumour washout. *Br J Radiol* 2011;84:403-12.
12. Willatt JM, Hussain HK, Adusumilli S, Marrero JA. MR Imaging of hepatocellular carcinoma in the cirrhotic liver: Challenges and controversies. *Radiology* 2008;247:311-30.
13. Taouli B, Koh DM. Diffusion-weighted MR imaging of the liver. *Radiology* 2010;254:47-66.

14. Seale MK, Catalano OA, Saini S, Hahn PF, Sahani DV. Hepatobiliary-specific MR contrast agents: Role in imaging the liver and biliary tree. *Radiographics* 2009;29:1725-48.
15. Bruix J, Sherman M, Practice Guidelines Committee, American Association for the Study of Liver Diseases. Management of hepatocellular carcinoma. *Hepatology* 2005;42:1208-36.
16. Pedrosa I, Alsop DC, Rofsky NM. Magnetic resonance imaging as a biomarker in renal cell carcinoma. *Cancer* 2009;115:2334-45.
17. Ng CS, Wood CG, Silverman PM, Tannir NM, Tamboli P, Sandler CM. Renal cell carcinoma: Diagnosis, staging, and surveillance. *AJR Am J Roentgenol* 2008;191:1220-32.
18. Jung SC, Cho JY, Kim SH. Subtype differentiation of small renal cell carcinomas on three-phase MDCT: Usefulness of the measurement of degree and heterogeneity of enhancement. *Acta Radiol* 2012;53:112-8.
18. Umeoka S, Koyama T, Miki Y, Akai M, Tsutsui K, Togashi K. Pictorial review of tuberous sclerosis in various organs. *RadioGraphics* 2008;28:e32.
20. Choyke PL, ACR Committee on Appropriateness Criteria. ACR Appropriateness Criteria on incidentally discovered adrenal mass. *J Am Coll Radiol* 2006;3:498-504.
21. Boland GW. Adrenal imaging: Why, when, what, and how? Part 2. What technique? *AJR Am J Roentgenol* 2011;196:W1-5.
22. Blake MA, Kalra MK, Sweeney AT, Lucey BC, Maher MM, Sahani DV, et al. Distinguishing benign from malignant adrenal masses: Multi-detector row CT protocol with 10-minute delay. *Radiology* 2006;238:578-85.
23. Kitajima K, Kaji Y, Imanaka K, Sugihara R, Sugimura K. MRI findings of uterine lipoleiomyoma correlated with pathologic findings. *AJR Am J Roentgenol* 2007;189:W100-4.
24. Loffroy R, Nezzal N, Mejean N, Sagot P, Krausé D. Lipoleiomyoma of the uterus: Imaging features. *Gynecol Obstet Invest* 2008;66:73-5.
25. Lalwani N, Prasad SR, Vikram R, Shanbhogue AK, Huettner PC, Fasih N. Histologic, molecular, and cytogenetic features of ovarian cancers: Implications for diagnosis and treatment. *RadioGraphics* 2011;31:625-46.
26. Gaskin CM, Helms CA. Lipomas, lipoma variants, and well-differentiated liposarcomas (atypical lipomas): Results of MRI evaluations of 126 consecutive fatty masses. *AJR Am J Roentgenol* 2004;182:733-9.
27. Rajiah P, Sinha R, Cuevas C, Dubinsky TJ, Bush WH Jr, Kolokythas O. Imaging of uncommon retroperitoneal masses. *RadioGraphics* 2011;31:949-76.
28. Chhabra A, Soldatos T. Soft-tissue lesions: When can we exclude sarcoma? *AJR Am J Roentgenol* 2012;199:1345-57.

**Source of Support:** Nil, **Conflict of Interest:** None declared.